

Supporting Information

Contents

Experimental section

Fig. S1. The schematic diagram of the proposed mechanism for the photo-induced production of **9-AC** molecular.

Fig. S2. The PXRD plots of triclinic **9-Ac** molecule before and after light irradiation.

Fig. S3. The color changes of triclinic **9-Ac** after Xe lamp light irradiation.

Fig. S4. IR spectra of triclinic **9-AC** in the KBr matrix: before and after irradiation.

Fig. S5. Temperature-dependent susceptibilities of triclinic **9-AC** under a dc magnetic field of 1000 Oe.

Fig. S6. The calculated spatial distributions of the HOMO (left) and LUMO (right) the of triclinic **9-AC** calculated at the B3LYP/6-311G(d) level.

Fig. S7. The ESR spectrum of triclinic **9-AC**[•] radicals upon standing in dark for 5 weeks at solid state.

Fig. S8. IR spectra of monoclinic **9-AC** in the KBr matrix: before and after irradiation.

Fig. S9. The H-bonding and π - π stacking interactions of **9-AC** for monoclinic form.

Fig. S10. The H-bonding and π - π stacking interactions of **9-AC** for triclinic form.

Fig. S11. IR spectra of **9-AC** (crystallized in methanol and water) in the KBr matrix: before and after irradiation.

Fig. S12. The PXRD plots of compound **1** before and after light irradiation.

Fig. S13. The TG plot of compound **1** under N₂ atmosphere.

Fig. S14. The color changes of compound **1** after Xe lamp light irradiation.

Fig. S15. IR spectra of compound **1** in the KBr matrix: before and after irradiation.

Fig. S16. Isothermal magnetization curve of **1** at 2 K before and after light irradiation.

Table S1. Mülliken charges of triclinic **9-AC**.

Table S2. Crystal data for **1** at 293 K.

Table S3. Selected bond lengths (Å) and angles (°) for **1** at 293K.

Table S4. The H-bond lengths (Å) for **1** at 293K.

Experimental Section

Materials and methods

9-anthracene carboxylic acid was purchased from Chemsoon (97%).

Synthesis of crystalline 9-AC:

The triclinic **9-AC** sample was prepared by recrystallization from methanol;¹ Elemental analysis (%): calcd for C₁₅H₁₀O₂ (222.24): C, 81.07; H, 4.54; O, 14.40. Found: C, 80.96; H, 4.44; O, 14.61. IR (KBr pellets, cm⁻¹): 3406(w), 3028(w), 2964(m), 2586(w), 1681(s), 1413(m), 1319(s), 1258(s), 1214(m), 1239(m), 954(s), 867(m), 780(w), 716(s), 621(m), 501(w). The monoclinic **9-AC** sample was prepared by recrystallization from ethyl acetate according to literature procedure;² Elemental analysis (%): calcd for C₁₅H₁₀O₂ (222.24): C, 81.07; H, 4.54; O, 14.40. Found: C, 81.35; H, 4.42; O, 14.52. IR (KBr pellets, cm⁻¹): 3406(w), 3028(w), 2964(m), 2586(w), 1681(s), 1413(m), 1319(s), 1258(s), 1214(m), 1239(m), 954(s), 867(m), 780(w), 716(s), 621(m), 501(w). Monoclinic and triclinic mixtures were obtained by dissolving the 9-Ac in a solution of methanol and water (2:1) and evaporation at room temperature. Elemental analysis (%): calcd for C₁₅H₁₀O₂ (222.24): C, 81.07; H, 4.54; O, 14.40. Found: C, 81.19; H, 4.36; O, 14.69. IR (KBr pellets, cm⁻¹): 3406(w), 3028(w), 2964(m), 2586(w), 1681(s), 1413(m), 1319(s), 1258(s), 1214(m), 1239(m), 954(s), 867(m), 780(w), 716(s), 621(m), 501(w).

Synthesis of 1:

A mixture of Ni(NO₃)₂·6H₂O (0.3 mmol, 0.087 g), 9-anthracene carboxylic acid (9-AC, 0.2 mmol, 0.044 g) and Triethanolamine (TEA, 0.1 mL) were dissolved in 3 mL of CH₃OH and 3 mL of H₂O. The resultant solution was sealed in a glass vial and heated to 110 °C for 4 days. Blue X-ray-quality crystals were formed and dried in air. Yield: 45% based on Ni(NO₃)₂·6H₂O. Elemental analysis (%): calcd for C₄₂H₄₈N₂NiO₁₀ (799.53): C, 63.09; H, 6.05; O, 20.01; N, 3.50. Found: C, 64.32; H, 5.98; O, 19.98; N, 3.34. IR (KBr pellet, cm⁻¹): 3260(w), 2610(w), 2586(w), 1941(w), 1790(w), 1554(s), 1430(s), 1385(m), 1308(s), 1148(m), 1067(s), 876(m), 743(s), 730(s), 650(w), 595(w), 514(w), 421(w).

Elemental analyses (C, H, O and N) were measured on a Perkin-Elmer 240C analyzer (Perkin-Elmer, USA). IR spectra were performed on a MAGNA-560 (Nicolet) FT-IR spectrometer with KBr pellets. The luminescence data were recorded on an F-4700 Fluorescence

spectrometer. The solid-state UV-Vis spectra were measured using BaSO₄ as a reference on a PerkinElmer Lambda-950 spectrophotometer. Electron spin resonance (ESR) spectroscopy was recorded on a Bruker E500 spectrometer. Thermogravimetric (TG) analyses were measured using a powder sample under N₂ atmosphere on a TG-DTA 8121 analyzer. Magnetic measurements of the polycrystalline samples of **9-Ac** after light irradiation was carried out on a Quantum Design SQUID (PPMS) magnetometer. Molecular orbital calculations were performed using the Gaussian 09 program and the basis set B3LYP/6-311G(d) method and adapted from the crystal X-ray data. Powder X-ray diffraction (PXRD) spectroscopy was performed on a Rigaku diffractometer with a Cu-target tube and a graphite monochromator. Simulation of the PXRD curve was carried out by the single-crystal data and diffraction-crystal module of the Mercury (Hg) program available free of charge *via* the Internet at <http://www.iucr.org>. For the light irradiation experiments, a Perfect Light PLS-SXE 300 Xe lamp (320–780 nm, 250 W, at least 180 min) was equipped to prepare the colored samples of UV-vis, PXRD, ESR and magnetic studies.

X-ray Crystallography.

The single-crystal X-ray diffraction data of **1** was collected on a Rigaku SCX-mini diffractometer at 293(2) K with Mo-K α radiation ($\lambda = 0.71073 \text{ \AA}$). Then using the SHELX-2016 software to solve the structure. Detailed crystallographic data for **1** was summarized in Table S2, and the selected bond lengths and angles were listed in Table S3. Full crystallographic data for **1** has been deposited with the CCDC (2063584).

References

[S1] Heller, E.; Schmidt, G. M. J. Topochemistry. Part XXXIII.† The Solid-State Photochemistry of Some Anthracene Derivatives, *Isr. J. Chem.* **1971**, *9*, 449–462.

[S2] Fitzgerald, L. J.; Gerkin, R. E. Anthracene-9-carboxylic Acid, *Acta Crystallogr.* **1997**, *C53*, 71–73.

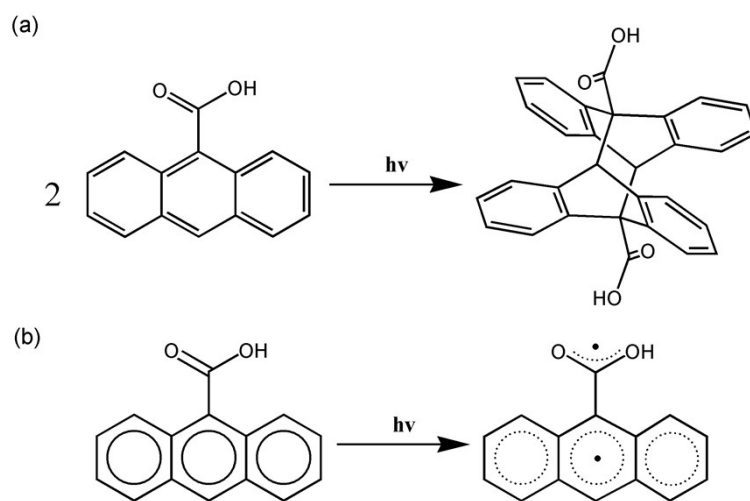


Fig. S1. The schematic diagram of the proposed mechanism for the photo-induced production of **9-AC** molecular.

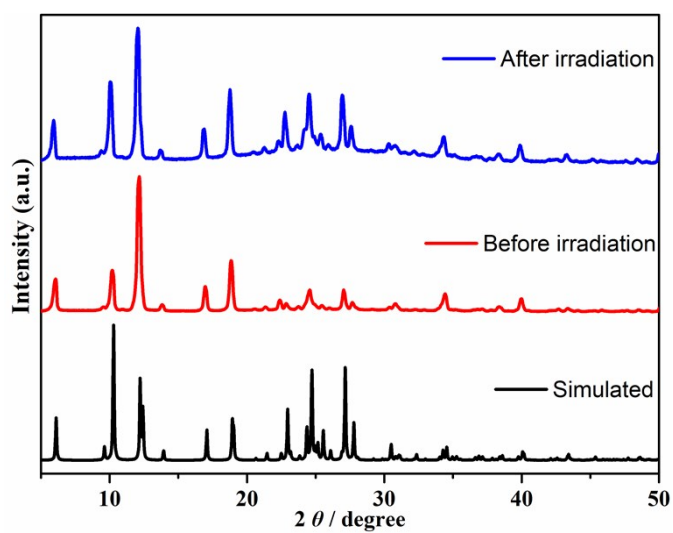


Fig. S2. The PXRD plots of triclinic **9-Ac** molecule before and after light irradiation.



Fig. S3. The color changes of triclinic **9-Ac** after Xe lamp light irradiation.

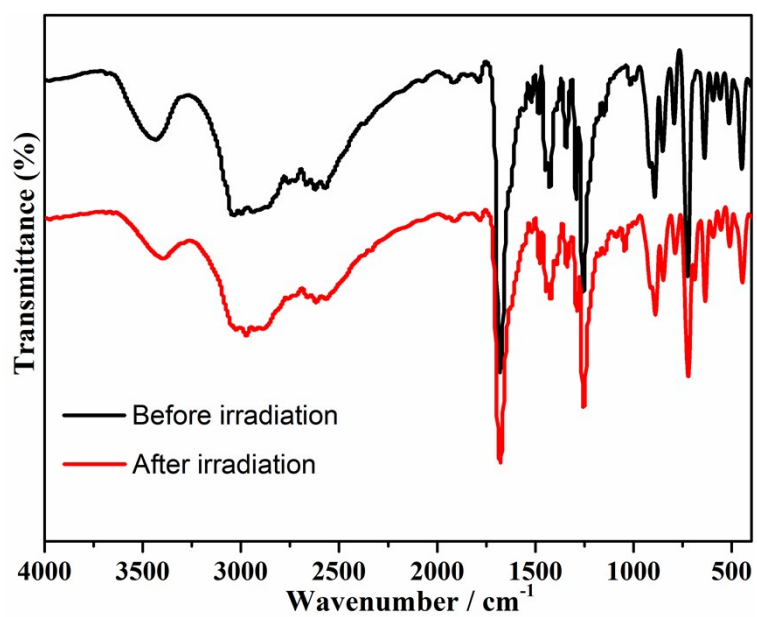


Fig. S4. IR spectra of triclinic **9-AC** in the KBr matrix: before and after irradiation.

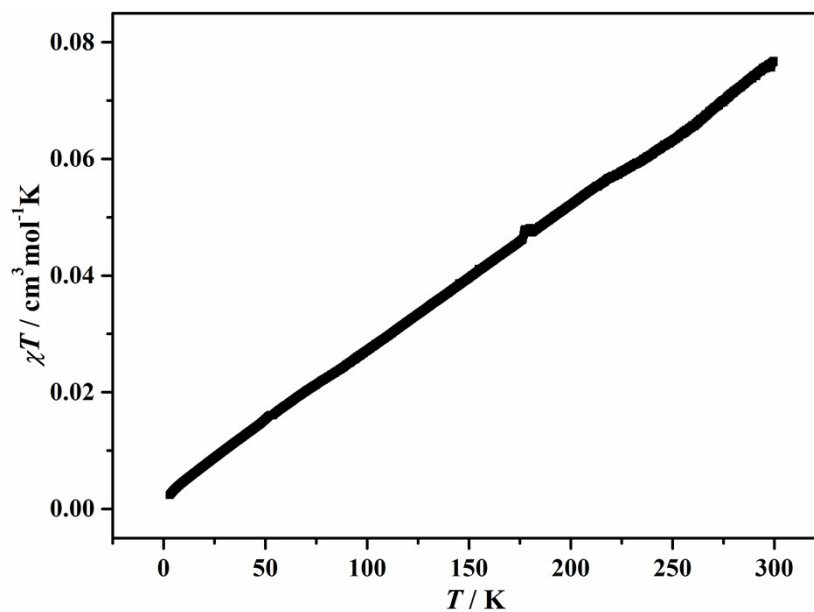


Fig. S5. Temperature-dependent susceptibilities of triclinic **9-AC** under a dc magnetic field of 1000 Oe.

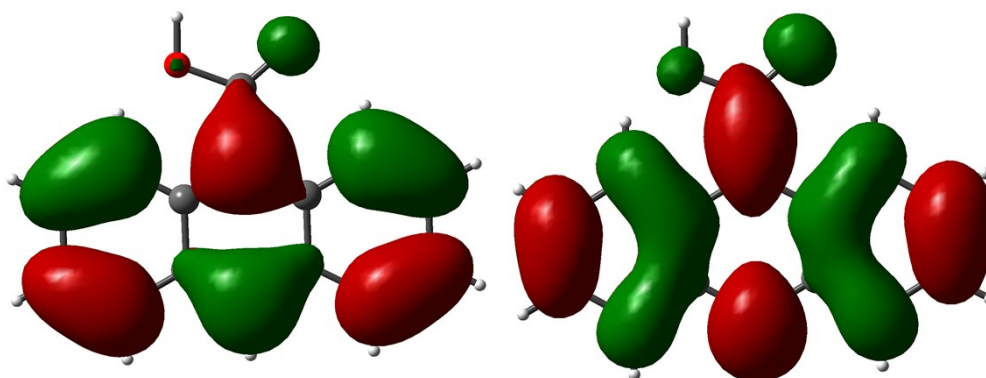


Fig. S6. The calculated spatial distributions of the HOMO (left) and LUMO (right) the of triclinic **9-AC** calculated at the B3LYP/6-311G(d) level.

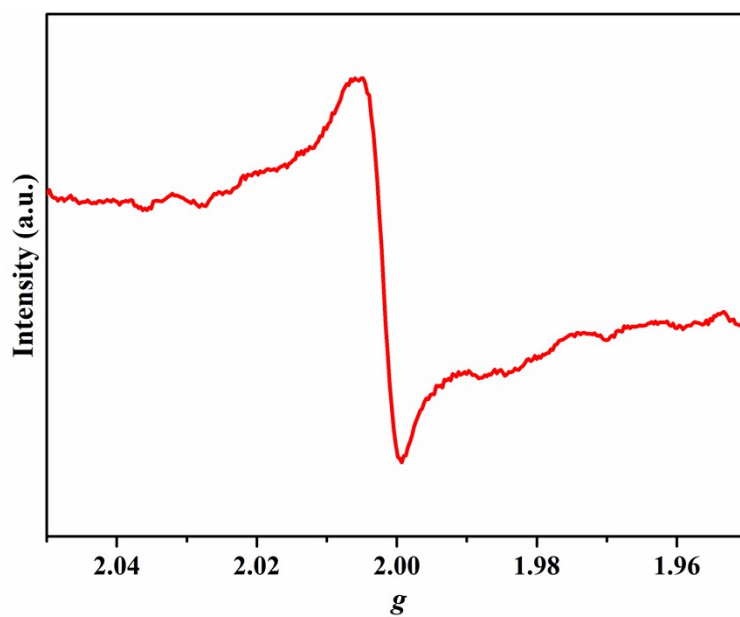


Fig. S7. The ESR spectrum of triclinic **9-AC**[•] radicals upon standing in dark for 5 weeks at solid state.

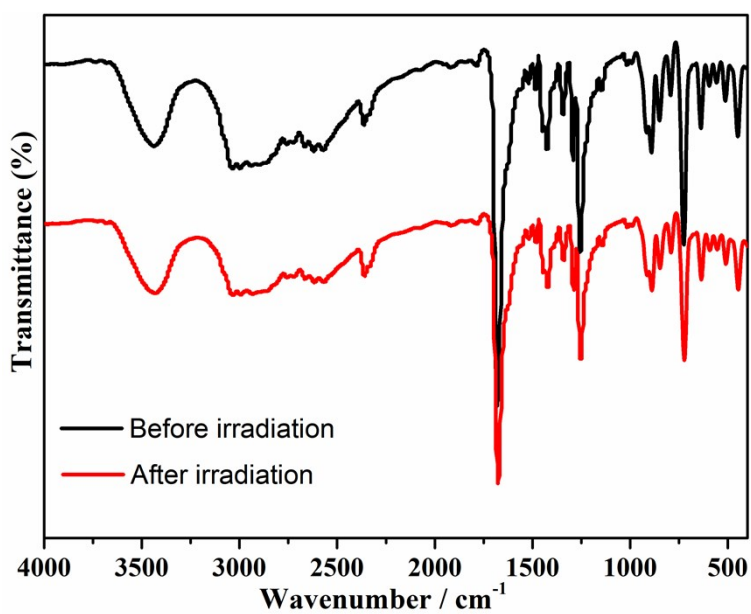


Fig. S8. IR spectra of monoclinic **9-AC** in the KBr matrix: before and after irradiation.

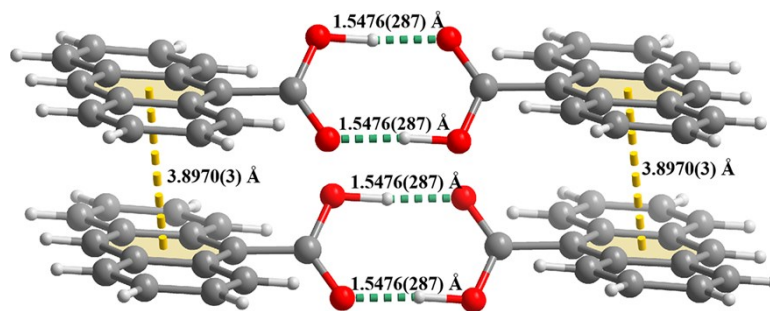


Fig. S9. The H-bonding and π - π stacking interactions of **9-AC** for monoclinic form.

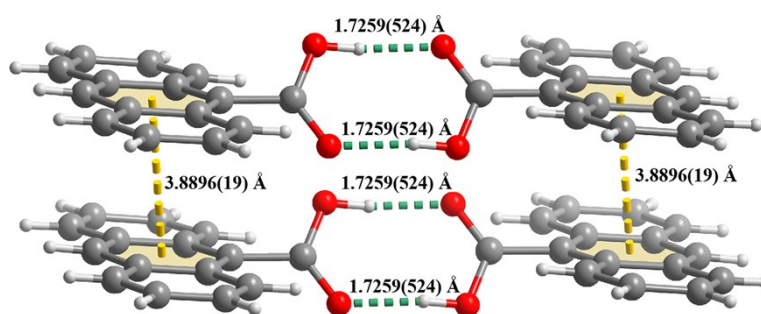


Fig. S10. The H-bonding and π - π stacking interactions of **9-AC** for triclinic form.

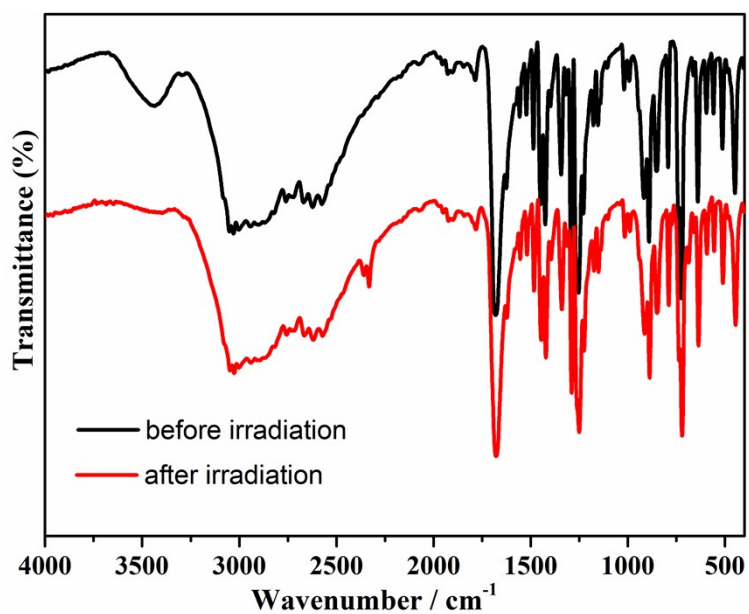


Fig. S11. IR spectra of **9-AC** (crystallized in methanol and water) in the KBr matrix: before and after irradiation.

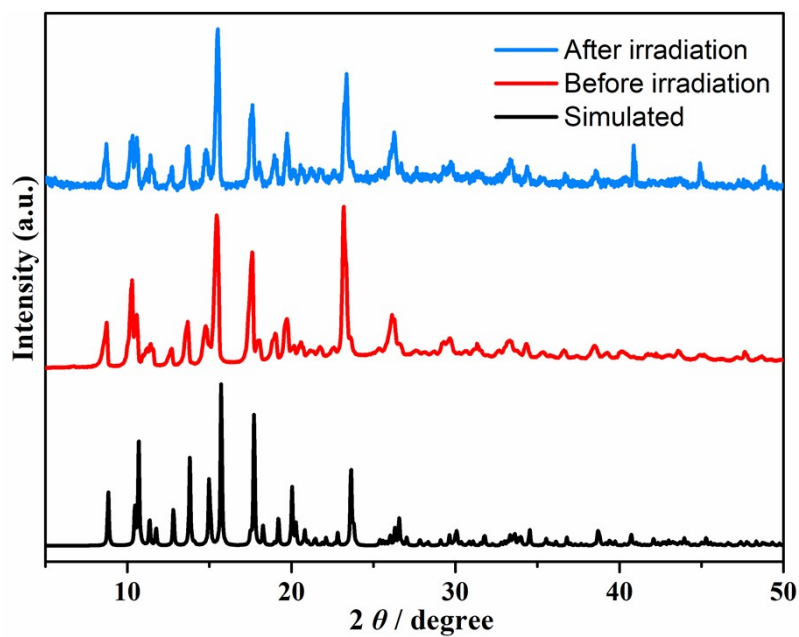


Fig. S12. The PXRD plots of compound **1** before and after light irradiation.

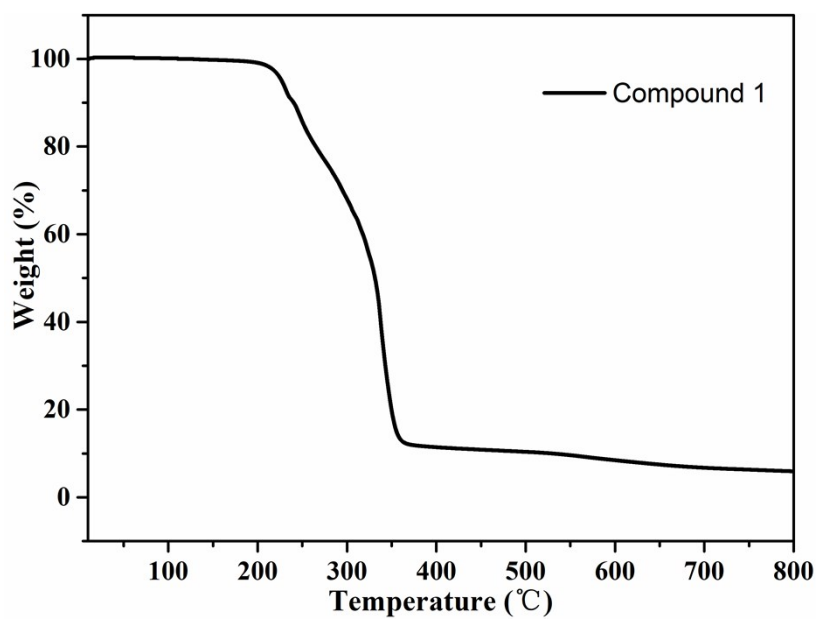


Fig. S13. The TG plot of compound **1** under N_2 atmosphere.



Fig. S14. The color changes of compound **1** after Xe lamp light irradiation.

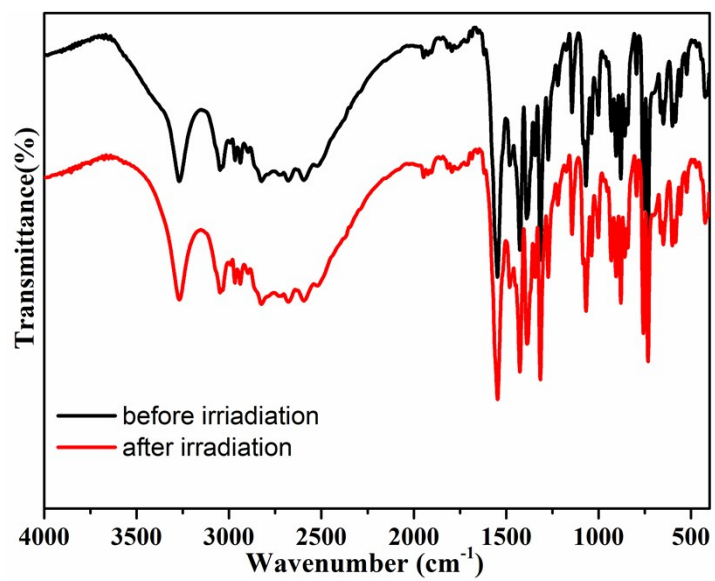


Fig. S15. IR spectra of compound **1** in the KBr matrix: before and after irradiation.

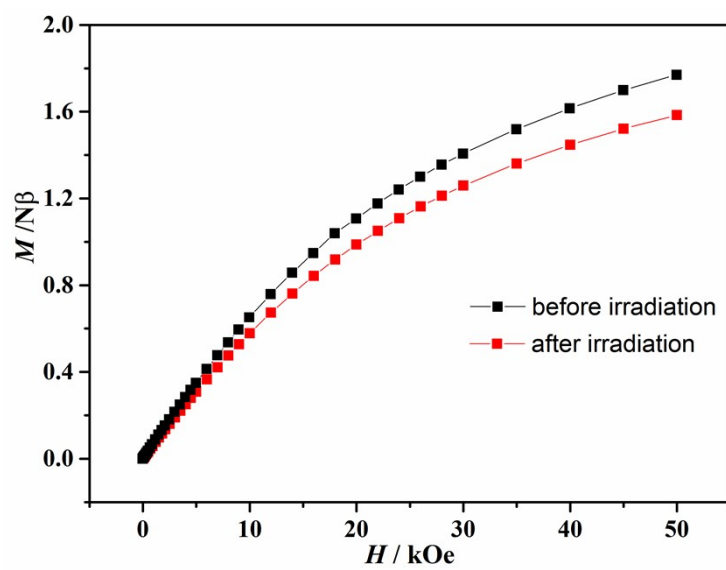
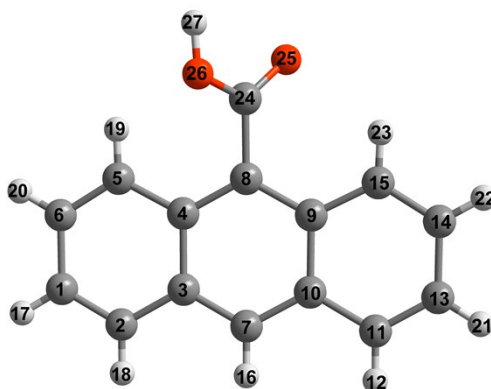


Fig. S16. Isothermal magnetization curve of **1** at 2 K before and after light irradiation.

Table S1. Mulliken charges of triclinic **9-AC**.



No.	Elements	Ground state
		Mulliken charges
1	C	-0.234781
2	C	-0.188473
3	C	-0.094446
4	C	-0.078039
5	C	-0.240316
6	C	-0.23826
7	C	-0.142346
8	C	-0.175722
9	C	-0.053526
10	C	-0.095552
11	C	-0.1845
12	H	0.240135
13	C	-0.237917
14	C	-0.22949
15	C	-0.241024
16	H	0.252849
17	H	0.237381
18	H	0.237786
19	H	0.384511
20	H	0.235856
21	H	0.240696
22	H	0.245327
23	H	0.328721
24	C	0.985015
25	O	-0.634494
26	O	-0.747666
27	H	0.428275

Table S2. Crystal data for **1** at 293 K.

1	
Formula	C ₄₂ H ₄₈ N ₂ NiO ₁₀
<i>Mr</i> (g·mol ⁻¹)	799.53
Crystal system	Monoclinic
Space group	<i>P</i> 2 ₁ / <i>n</i>
<i>a</i> /Å	9.2120(15)
<i>b</i> /Å	16.537(2)
<i>c</i> /Å	13.109(3)
<i>α</i> /°	90
<i>β</i> /°	106.649(18)
<i>γ</i> /°	90
<i>V</i> /Å ³	1913.3(6)
<i>Z</i>	2
<i>D_c</i> /g cm ⁻³	1.388
<i>μ</i> /mm ⁻¹	0.569
<i>F</i> (000)	844.0
<i>R</i> _{int}	0.0381
limiting indices	-10 ≤ <i>h</i> ≤ 10, -19 ≤ <i>k</i> ≤ 19, -5 ≤ <i>l</i> ≤ 15
Total reflections	6541
Unique reflections	3364
<i>R</i> ₁ , <i>wR</i> ₂ [<i>I</i> > 2σ(<i>I</i>)]	0.0455 0.1238
<i>R</i> ₁ , <i>wR</i> ₂ [all data]	0.0613 0.1352
GOF on <i>F</i> ²	1.048

Table S3. Selected bond lengths (Å) and angles (°) for **1** at 293K.

1			
Ni(1)-O(3)#1	2.046(2)	C(7)-C(12)	1.432(4)
Ni(1)-O(3)	2.046(2)	C(8)-C(9)	1.350(5)
Ni(1)-O(2)#1	2.0584(19)	C(9)-C(10)	1.410(5)
Ni(1)-O(2)	2.0584(19)	C(10)-C(11)	1.337(5)
Ni(1)-N(1)#1	2.085(2)	C(11)-C(12)	1.417(5)
Ni(1)-N(1)	2.085(2)	C(12)-C(13)	1.386(5)
C(1)-N(1)	1.485(3)	C(13)-C(14)	1.379(5)
C(1)-C(2)	1.521(4)	C(14)-C(15)	1.424(4)
C(2)-O(1)	1.391(4)	C(14)-C(19)	1.439(4)
C(3)-C(4)	1.475(6)	C(15)-C(16)	1.339(5)
C(3)-N(1)	1.500(4)	C(16)-C(17)	1.407(5)
C(4)-O(2)	1.437(4)	C(17)-C(18)	1.368(4)
C(5)-N(1)	1.463(5)	C(18)-C(19)	1.414(4)
C(5)-C(6)	1.514(4)	C(19)-C(20)	1.405(4)
C(6)-O(3)	1.436(4)	C(20)-C(21)	1.522(3)

C(7)-C(20)	1.386(4)	C(21)-O(5)	1.243(3)
C(7)-C(8)	1.425(4)	C(21)-O(4)	1.251(3)
O(3)#1-Ni(1)-O(3)	180	O(1)-C(2)-C(1)	110.0(3)
O(3)#1-Ni(1)-O(2)#1	92.06(8)	C(4)-C(3)-N(1)	110.5(3)
O(3)-Ni(1)-O(2)#1	87.94(8)	O(2)-C(4)-C(3)	109.5(3)
O(3)#1-Ni(1)-O(2)	87.94(8)	N(1)-C(5)-C(6)	112.2(3)
O(3)-Ni(1)-O(2)	92.06(8)	O(3)-C(6)-C(5)	108.1(3)
O(2)#1-Ni(1)-O(2)	180.00(8)	O(5)-C(21)-O(4)	124.4(2)
O(3)#1-Ni(1)-N(1)#1	82.83(9)	O(5)-C(21)-C(20)	119.0(2)
O(3)-Ni(1)-N(1)#1	97.17(9)	O(4)-C(21)-C(20)	116.6(2)
O(2)#1-Ni(1)-N(1)#1	83.93(10)	C(5)-N(1)-C(1)	109.4(3)
O(2)-Ni(1)-N(1)#1	96.07(10)	C(5)-N(1)-C(3)	112.0(3)
O(3)#1-Ni(1)-N(1)	97.17(9)	C(1)-N(1)-C(3)	113.2(2)
O(3)-Ni(1)-N(1)	82.83(9)	C(5)-N(1)-Ni(1)	103.31(18)
O(2)#1-Ni(1)-N(1)	96.07(10)	C(1)-N(1)-Ni(1)	111.85(17)
O(2)-Ni(1)-N(1)	83.93(10)	C(3)-N(1)-Ni(1)	106.7(2)
N(1)#1-Ni(1)-N(1)	180	C(4)-O(2)-Ni(1)	105.61(19)
N(1)-C(1)-C(2)	118.0(2)	C(6)-O(3)-Ni(1)	113.24(18)

Symmetry codes: #1 -x+1,-y+2,-z+2

Table S4. The H-bond lengths (Å) for **1** at 293K.

D-H...A	<i>d</i> (D-H) (Å)	<i>d</i> (H...A) (Å)	<i>d</i> (D...A) (Å)	∠(DHA) (deg)
O(1)-H(1)···O(4)	0.82	1.90	2.679(3)	159
O(2)-H(2)···O(4)	0.85(4)	1.75(4)	2.594(3)	169(4)
O(3)-H(3)···O(5)	0.75(4)	1.88(4)	2.621(3)	171(3)